Materials Science & Engineering A 577 (2013) 147–157

Contents lists available at SciVerse ScienceDirect

Materials Science & Engineering A

journal homepage: www.elsevier.com/locate/msea

Mechanical behavior under cyclic loading of the 18R-6R high-hysteresis martensitic transformation in Cu-Zn-Al alloys with nanoprecipitates

Franco de Castro Bubani [a,b,c], Marcos Sade [a,b,c,*], Francisco Lovey [a,c]

[a] Centro Atómico Bariloche (CNEA), Av. E. Bustillo Km. 9, 5 (8400) S.C.de Bariloche, Argentina
[b] CONICET, Buenos Aires, Argentina
[c] Instituto Balseiro, Universidad Nacional de Cuyo, Bariloche, Rio Negro, Argentina

ARTICLE INFO

Article history:
Received 19 October 2012
Received in revised form
5 April 2013
Accepted 8 April 2013
Available online 17 April 2013

Keywords:
Shape-memory alloys
Mechanical characterization
Martensitic transformations
Strain measurement

ABSTRACT

Mechanical damping applications could benefit from the large hysteresis, large pseudoelastic strain and the fact that the transformation stresses of the 18R↔6R martensite–martensite transformation depend very little on temperature in Cu-based alloys. This work presents the 18R↔6R mechanical cycling behavior of CuZnAl shape-memory alloy single crystals with electronic concentration $e/a=1.48$. A fine distribution of gamma phase nanoprecipitates is introduced to prevent plastic deformation of the 6R phase. Results show that, although significant 6R stabilization is observed at very low frequencies (below 10^{-2} Hz), it is possible to obtain more than 1000 stable pseudoelastic cycles with only minor changes in transformation stresses and hysteresis width at frequencies above 10^{-1} Hz. A more pronounced decrease in transformation stresses is observed after 1000 cycles. Nevertheless, the decrease in hysteresis is small up to 2000 cycles. Reported and present results indicate that pair interchange of atoms can explain the stabilization of 6R under quasistatic experimental conditions. However, at higher frequencies of cycling, stabilization of this martensite shows additional features, leading to a dynamic stabilization with slight effects on the mechanical behavior at the required frequency and number of cycles. On the whole, the behavior of this transformation is unique and very promising.

1. Introduction

The 6R phase in Cu-base shape-memory alloys (SMA) can be mechanically induced by applying a tensile stress to the 18R martensite, which in turn can be induced in the same way from the austenitic β phase, i.e., the metastable ordered structure resulting from the rapid cooling of the bcc high temperature phase, in which the type of order depends on the alloy composition [1–6]. These martensitic stress induced transformations are characterized by a mechanical hysteresis which is suitable for damping applications [7–16].

Several studies have been carried out for many years to analyze the significant parameters that characterize the stress induced transformations. NiTi and CuAlBe have been considered as interesting options for this type of applications. Most reported studies have focused their attention on the austenite–martensite transition, i.e., B2–B19′ in NiTi [11,17–22] the DO_3-18R in CuAlBe [13,23–25] or the $L2_1$-18R [26] in CuZnAl alloys embedded in glass fiber composites.

In CuZnAl it was shown that, by applying a tensile stress, two sequential reversible martensitic transformations β–18R and 18R–6R can produce more than 20% strain as pseudoelasticity [1,2,5,27,28]. Moreover, the mechanical cycle can be restricted to the 18R↔6R transformation showing two major differences from the β↔18R pseudoelastic cycles:

(i) The transformation–retransformation stresses show a weak dependence on temperature; $d\sigma/dT$ in 18R↔6Rtransformation might reach up to −0.42 MPa/K, depending on the crystal orientation [1,29–31]. On the other hand, a value of $d\sigma/dT \geq 2$ MPa/$K$is obtained for the β↔18R transition in Cu-based SMA [21]. This advantage becomes even more evident when compared with the value of $d\sigma/dT = 6.3$ MPa/K in NiTi alloys [21]. This is a very important property regarding applications where the surrounding temperature can change several tens of degrees.

ii) The larger hysteresis in the 18R↔6R transformation cycle, with a recoverable strain of about 10%, can also be an important advantage for some applications, i.e. damping devices for civil structures, such as buildings and bridges, to smooth out the oscillations produced by earthquakes, winds, etc.; it has been a subject of increasing interest in the last decades [5,32,33].

Recently, huge superelasticity has been reported in Fe-base alloys [34,35]. A highly textured Fe-base superelastic alloy, with

* Corresponding author at. Physics Department, Centro Atomico Bariloche (CNEA), Metal Physics Group, Av. E. Bustillo Km. 9, 5 (8400), 8400 S.C.de Bariloche, Rio Negro, Argentina Tel.: +54 2944 445265; fax: +54 2944 445290.
E-mail addresses: franco@cab.cnea.gov.ar (F. de Castro Bubani), sade@cab.cnea.gov.ar, marcossade05@yahoo.com.ar (M. Sade), lovey@cab.cnea.gov.ar (F. Lovey).

0921-5093/$ - see front matter © 2013 Elsevier B.V. All rights reserved.
http://dx.doi.org/10.1016/j.msea.2013.04.037

composition Fe-28.85Ni-17.59Co-5.45Al-7.94Ta-0.0095B (wt%) containing ordered Ni–Al bcc precipitates was presented by Tanaka et al. In a single cycle, the hysteresis of these alloys is greater than in the 18R–6R transformation in CuZnAl single crystals, which makes them potential candidates for seismic damping. However, shape recovery is not complete, and it is also important to assess the mechanical behavior of these textured alloys under cycling conditions. Some results concerning the cyclic behavior of a single crystal of an alloy very similar to the one invented by Tanaka et al. have been recently published by Krooss et al. [36], up to 100 cycles. In these Fe-base single crystals, hysteresis is considerably smaller than in the textured alloy and is comparable to the one observed in 18R–6R transformation in CuZnAl single crystals. Other interesting Fe-base alloy was reported by Omori et al. This alloy with composition Fe-34Mn-15Al-7.5Ni (wt%) shows pseudoelasticity in the temperature range from 223 K to 423 K, and a slight temperature dependence of the critical stress to obtain the martensitic transformation, in fact close to the one obtained for the 18R–6R transformation in Cu based alloys. These new Fe-base superelastic alloys are very promising for earthquake damping, but more studies are required for a thorough assessment of dynamic behavior under earthquake conditions.

One of the associated difficulties to consider the 18R–6R martensitic transformation in CuZnAl alloys is the reported plastic deformation of the 6R martensite, which happens at approximately the same stress level at which the martensite–martensite transformation takes place [37]. A first approach to solve this problem was presented in [38]. It was found that nanoprecipitates, due to precipitation hardening, can greatly improve the mechanical behavior of adequately-oriented CuZnAl single crystals. The plastic deformation of the 6R phase is minimized or completely suppressed. A new alternative can then be considered, taking into account the fact that the 18R–6R phase transition in Cu-based alloys shows certain features which are advantageous for potential applications, such as wide hysteresis and very weak dependence of the transformation stresses on temperature.

Another fact to be considered for applications of the 18R–6R transition in Cu-based shape-memory alloys is the martensitic stabilization effect. The stabilization of martensite is usually described as the increase in critical transformation temperatures or, equivalently, the decrease in critical stresses if the transition is mechanically induced [39–46].

It is clear that stabilization might affect any device using a shape memory alloy in case it is not controlled or well considered in the lifespan of an application. Very briefly, explanations on the martensitic stabilization might be classified in two different types: those which consider changes in atomic configuration of the martensite after aging and those which justify shifts in critical temperatures or stresses as a consequence of pinning phenomena [40,47–49]. Indeed, a large amount of results has been reported in the last decades concerning the effect of aging in the martensitic structure. Different phenomena have been considered; stabilization of martensite and the rubber-like effect are probably the main focus of these studies. An interesting and general approach to the problem was presented by Otsuka and Ren [50,51]. The proposition of these authors, named SC-SRO (from Symmetry Conforming-Short Range Order), mainly considers that, at the equilibrium stage, the probability of finding a second point defect around a first one possesses the same symmetry as the crystal symmetry. In this way, if a martensitic transition takes place and diffusion is allowed in the martensitic structure, an evolution of the short range order will take place to reach a stable atomic configuration which conforms to the symmetry of the martensite. This model allows of the comprehension of stabilization phenomena both in equilibrium martensitic structures and in non-equilibrium ones. The same authors consider that CuZnAl alloys constitute an example of martensitic transitions which lead to a non-equilibrium martensite, which can lower its free energy by a significant contribution of long range order evolution in addition to their suggested mechanism. Particularly, the stabilization of 18R martensite in CuZnAl has been analyzed in depth by Abu Arab and Ahlers [42]. These authors explain the observed stabilization in stress induced martensitic single crystals by a pair interchange between Cu and Zn atoms which in fact decreases the free energy of the martensite, leading to a more stable structure. This mechanism, which requires diffusion to be activated and uses the available data of pair interchange energies, clearly explains the observed effects in this system. Additionally, an increase in the degree of disorder during aging in martensite has been experimentally measured in CuZnAl alloys by Hashiguchi et al., using a four circle diffractometer [52]. Due to the mentioned facts, taking into consideration that martensite in these alloys is not an equilibrium phase when it is thermally or stress induced, and considering the excellent agreement between experimental results concerning either kinetics or amount of stabilization and the model of Cu–Zn pair interchange, in the present manuscript we will consider the mechanism suggested by Abu Arab et al. as the main contribution to the stabilization effect.

As the present work focuses on the 18R–6R stress induced transformation, it is necessary to analyze the effect of 6R stabilization on the mechanical behavior associated with this transition. As a start point, similar considerations can be performed to analyze aging phenomena in 18R and 6R martensite. On one hand, neither the 18R nor the 6R martensite is a stable phase when it is induced, and an evolution of the free energy of the 6R structure is expected to take place if diffusion is allowed. On the other hand, the crystalline structure is sufficiently different if both martensites are compared. Only a reduced amount of works considering the stabilization of 6R have been published and some outputs will be briefly commented below.

Saule et al. [32,53,54] studied the stabilization of martensitic phases in CuZnAl alloys and found out that 6R stabilization is faster than 18R stabilization under static conditions. The main difference between the stabilization of 18R and 6R martensites arises from the higher symmetry of the 6R structure, which is close to an fcc structure if order is disregarded. This difference makes the interchange of Cu and Zn atoms possible on additional planes with the same symmetry of the basal plane [32,55]. This is potentially troublesome if one intends to avoid 6R stabilization altogether, as the time spent in 6R should be minimized.

However, it should be noted that most of the reported results on stabilization of martensite were obtained under experimental conditions far from the required ones at seismic events. Just as an example, most of the results obtained by Abu Arab and Ahlers [42] and by Saule et al. [32,53,54] were obtained by tensile inducing transitions to obtain either an 18R single crystal or a 6R single crystal and letting the martensite age under stress, at constant temperature, for different times. The amount of stabilization in these martensitic single crystals has been determined mainly by measuring the decrease in the critical stress to obtain the retransformation to austenite, in the former transition, or to 18R, in the latter one.

A previous study [56] has found that the kinetics of dynamic 18R martensite stabilization observed under mechanical β–18R cycling in CuZnAl alloys cannot be satisfactorily described by static stabilization models. Several physical phenomena are involved in the dynamic stabilization of martensite during transformation–retransformation cycling, making it considerably more complex than static stabilization [56–58]. As an example, we can mention that pseudoelastic cycling between the $L2_1$ austenitic phase and the 18R structure at temperatures higher than room temperature can be well explained by considering just two phenomena: the stabilization of martensite and the recovery of the order of the austenitic structure [56]. Yawny et al. reported that the kinetics of

both diffusive phenomena measured under quasistatic conditions do not satisfactorily explain the evolution of the mechanical behavior of the material [56]. This has led to the interesting fact that 18R martensite stabilization kinetics is increased during pseudoelastic cycling at frequencies far from quasistatic conditions. Therefore, one should not expect the dynamic stabilization kinetics of 6R martensite to match static stabilization and one of the aims of the present manuscript is to improve the comprehension of this matter.

Finally, it should be noticed that seismic events or even other damping phenomena usually require good performance of the material concerning cycling. Moreover, according to specific requirements, particular frequencies should be considered. In order to establish whether the 18R↔6R pseudoelastic cycle in CuZnAl SMA would be useful for various applications such as in actuators, robotics, damping devices, etc., more knowledge of the behavior of this transformation under different mechanical cycling conditions is required.

This work focuses on the mechanical behavior of the 18R↔6Rtransformation in CuZnAl single crystals with nanoprecipitates, submitted to mechanical cycling, with particular regards to seismic engineering applications. Different frequencies are considered and the effect of 6R martensite stabilization is analyzed.

2. Experimental procedure

Several Cu-14.78 at%Zn–16.61 at%Al (Cu-16.743Zn-7.762Al in wt %) cylindrical single crystals were grown by using the Bridgman method, all with electronic concentration $e/a=1.48$ and nominal 18R martensitic transformation temperature $M_s=273$ K. The alloy composition was chosen so as to optimize both the manufacturing process and the β–18R martensitic transformation temperature: the electronic concentration of 1.48 corresponds to the maximum stability of the austenitic (β) phase and, at this e/a value, it is considerably simpler to manufacture single crystals without austenite decomposition. The M_s temperature of the alloy was chosen so as to allow for a wide range of working temperatures in seismic devices: above M_s, both the β–18R and the 18R–6R transformations can be potentially employed in a damping device. At temperatures below M_s, the 18R–6R transformation can be used.

A seed was used so that all crystals have the same orientation (Fig. 1). The orientation chosen maximizes the Schmid factor of the 18R–6R transformation, minimizing the transformation stress. This is done in order to prevent plastic deformation of the 6R phase. A discussion on the effects of the orientation on the 18R–6R transformation can be found in [38].

Cylindrical single crystals, with a diameter of approximately 4.7 mm were produced. Samples were then obtained by mechanically machining the single crystals to 2.5 mm diameter. After machining, samples were submitted to a precipitation thermal treatment which consists in keeping samples at 1103 K for 30 min, followed by air cooling to 803 K and quenching in water at 278 K. This thermal treatment, called step-quenching, has been studied in previous works [59,60] and is known to produce a uniform distribution of γ phase nanoprecipitates in the alloy during the water quenching phase. The γ phase is a hard intermetallic compound. The precipitate density, averaged at three different points, is $\rho=(7\pm3)\times10^{-7}$ nm^{-3}. The average precipitate radius is $r=(11\pm2)$ nm. The precipitates are coherent with the β matrix [38]. The precipitates formed by quenching are out-of-equilibrium phases observed in the equilibrium phase diagram. However, it has been shown by Lovey et al. [61], that these small precipitates correspond to Cu_5Zn_8 γ–brass type precipitates belonging to the $I\bar{4}3m$space group, having a cubic structure with 52 atoms in the unit cell, as determined much earlier by Bradley and Gregory [62].

After the thermal treatment, samples were ground with 600 grit sandpaper and polished electrochemically with a solution of 15% nitric acid in methanol. Further details on specimen preparation can be found in [38]. The tensile orientation of the crystals used is given in Fig. 1, together with a complete β–18R–6R reference cycle which was obtained for a sample with the same composition and tensile axis as those samples mentioned in Table 1.

Several tensile samples were prepared and cycled at different frequencies.

At frequencies below 0.2 Hz, an Instron 5567 Machine (or Instron 1123, updated to model 5567) was used to test samples. At 1 Hz, a MTS 810 machine was used. Some curves were obtained with an Instron 2620-602 extensometer and others with crosshead displacement, the specific method used to measure strain is

Table 1
Samples and frequencies used. Samples A, B, C and D were submitted to pseudoelastic cycling at the stated frequency. Samples E and F were used to determine the quasistatic stabilization of the 6R martensite. Details in the text.

Sample	Crystal	Frequency (Hz)
A	1	1.9×10^{-2}
B	2	0.147
C	3	1.0
D	4	8.35×10^{-2}
E	5	Quasistatic stab
F	5	Quasistatic stab

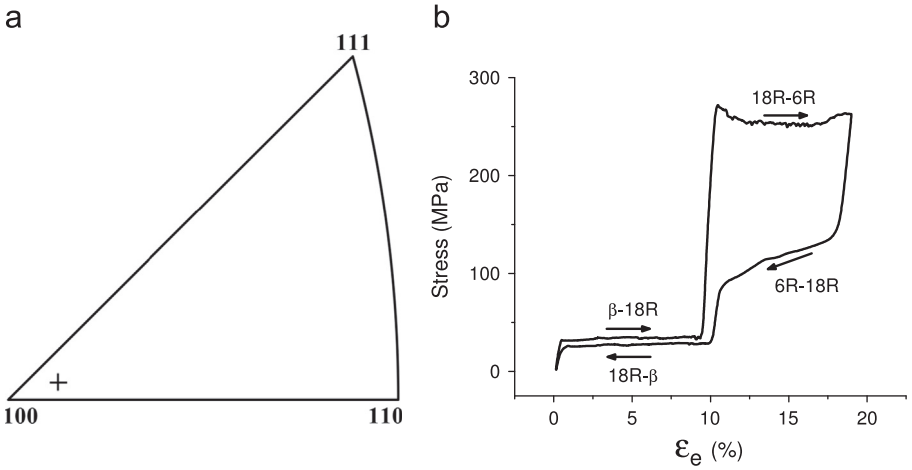

Fig. 1. (a) Orientation of the tensile axis of the crystals used; (b) reference β–18R–6R stress–strain cycle. $T=303$ K; $v=0.3$ mm/min.

described individually for each curve. The strain obtained from extensometer data will be named ε_e and the strain obtained from crosshead movement data will be named ε_c. The β-phase initial length is taken as the zero-strain reference in all curves unless otherwise stated.

Different crosshead speeds were used in order to assess the effects of the different stabilization constants of the 18R and 6R martensites. The maximum frequency used is 1 Hz, which is the same order of magnitude of earthquake oscillation frequencies [16].

During cycling at a constant frequency, it is possible to quantify the shift in critical transformation stresses for a given strain ε as the difference in transformation stress between the reference cycle, $\sigma_r(\varepsilon)$, and the nth cycle, $\sigma_n(\varepsilon)$, i.e. $\Delta\sigma = \sigma_r(\varepsilon) - \sigma_n(\varepsilon)$. This method can be used to describe the stress shift caused by 6R martensite stabilization and is valid either for the 18R–6R transformation or the 6R–18R retransformation; a supra index will be used when necessary. The second 18R–6R transformation is used in the present work as the reference transformation from which $\sigma_r(\varepsilon)$ is determined, since the first transformation in some cases shows artifacts which make it more difficult to accurately determine stress data. However, when necessary, variations of the critical stress from the first 18R–6R transformation will be specifically stated. A positive $\Delta\sigma$ will then describe a decrease in the critical stress to obtain the 6R by tensile loading the sample, or the 18R martensite during unloading. In order to take into account the contribution of the elastic deformation, the variation of the stresses corresponding to a fixed amount of transformation is measured as the intersection of a straight line parallel to the 18R elastic range of the stress–strain curve and the curve at the transformation stage.

Additional experiments have been performed to get some insight on the quasistatic behavior of the 6R stabilization effect at a concentration of vacancies close to or somewhat smaller than the concentration used for dynamic tests. In these quasistatic experiments, partial 18R–6R transformations were obtained and the strain (amount of 6R formed) was kept fixed for selected time intervals at different percentages of 18R–6R transformation and finally retransformed to 18R. From the shift of the transformation stresses as compared to the original values, it was possible to determine the stabilization kinetics of 6R martensite, as performed by Saule et al. [32,53] for the same martensite and by Abu Arab and Ahlers for the 18R martensite [42].

3. Experimental results

3.1. Behavior under mechanical cycling at different frequencies and temperatures

The dynamic (cyclic) behavior of the material was first determined by low-speed cycling at 303 K. In this test the sample undergoes only one β–18R transformation. The 18R phase is further strained and the sample is mechanically cycled through the 18R–6R transformation at 303 K, see the first cycle in Fig. 2a. The 18R–6R transformation starts with a yield point at around 292 MPa, as shown in Fig. 2a. A partial 18R–6R transformation was induced (42%) between ε_0 and ε_{max} as indicated in Fig. 2a and b. On unloading in Fig. 2a the specimen retransforms from 6R to 18R until the stress drops to a value equal to the 18R–β retransformation stress. This incomplete retransformation was reported in [38] and was tentatively attributed to thin 6R lamellae retained in the 18R martensite. The start point for further cycling is shown as point A in the curve (Fig. 2a). The crosshead speed used up to point A is 0.3 mm/min. After reaching point A, the crosshead speed was increased to 2.052 mm/min and cycling started at 1.9×10^{-2} Hz. In the beginning of the cycling experiment, the whole 18R–6R cycle lies at stresses above the β–18R transformation stress as is clearly observed in Fig. 2a. The 18R–6R transformation and retransformation stresses drop in each cycle, and the slope of the transformation stress increases. After a certain number of cycles, the 6R–18R retransformation stress in part of the sample drops to a value below the 18R–β retransformation stress. This part of the sample

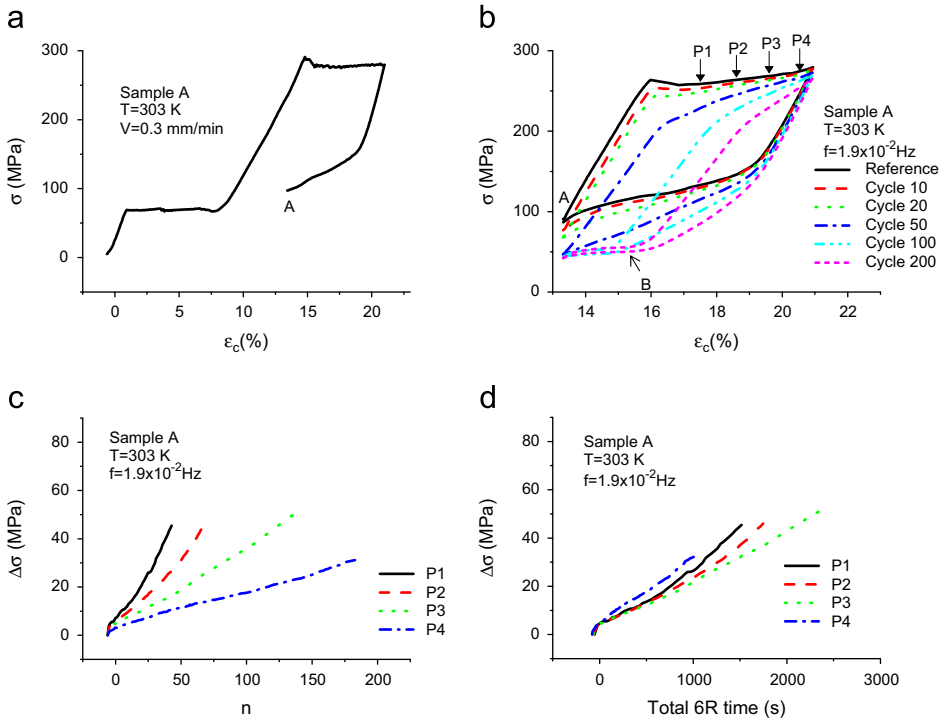

Fig. 2. sample A. (a) First load application and retransformation to point A. (b) 18R–6R low speed cycles starting from point A (same as in Fig. 2a), point B marks the onset of 18R–β retransformation in cycle 100. (c) 18R–6R transformation stress vs. number of cycles for different strain values. (d) 18R–6R transformation stress vs. accumulated time in 6R.

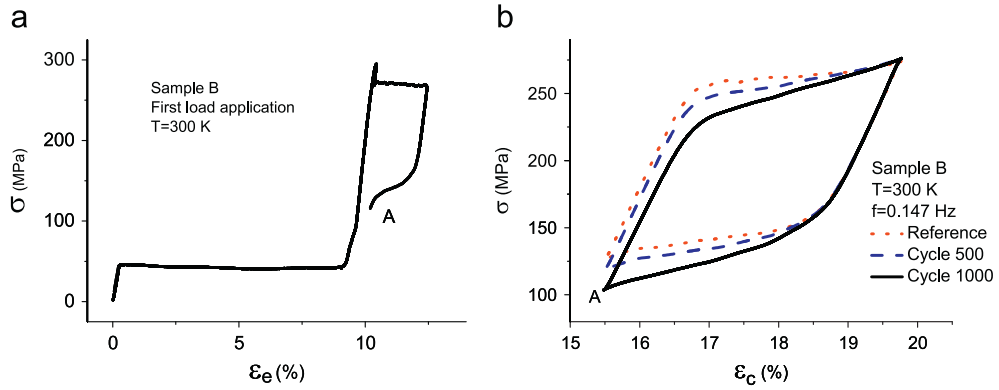

Fig. 3. (a) First load application (with extensometer), (crosshead speed = 0.3 mm/min), (b) cycling at 0.147 Hz (crosshead speed = 15 mm/min).

remains in 6R and no longer retransforms to 18R in each cycle, as 18R–β retransformation starts to take place elsewhere in the sample, limiting further stress drops. This phenomenon can be observed in Fig. 2b.

The 18R–6R transformation stress for several different strain values was measured in each cycle. The elasticity of the system has been considered and corrected in the measurement process. The variation of the transformation stresses $\Delta\sigma$ for the 18R–6R transition, as defined in Section 2, was determined and plotted as a function of the number of cycles (Fig. 2c) and as a function of the accumulated time interval the corresponding portion of the sample spends in 6R. Different portions of the sample are identified by the amount of 18R–6R transformation given in % (see arrows P1 to P4 in Fig. 2b). Some small differences in the stabilization vs. time curves are observed in Fig. 2d. for the various transformed regions of the sample. The reasons of such differences are not clear yet, they could be related to small changes in the sequences of the thin 6R plates as the 18R–6R transformation proceeds.

A sample from the same crystal was then submitted to cycling at a higher frequency (0.147 Hz, up to about 36% of 6R formation), at a test temperature of 300 K. Results are shown in Fig. 3. The first transformation curve obtained at a crosshead speed equal to 0.3 mm/min is presented in Fig. 3a. 'A' marks the point where cycling started. Crosshead speed is increased to 15 mm/min (frequency = 0.147 Hz) after this point is reached and then kept constant during the cycling stage. The interesting point here is that the observed change in the critical transformation stresses is smaller and the rate at which these stresses drop with the number of cycles is remarkably slower at this frequency. In fact, it is possible to reach 1000 cycles with relatively little difference in 18R–6R transformation and retransformation stresses, see Fig. 3b.

An important point in the low and intermediate frequency experiments presented in Figs. 2 and 3 is that the stress to transform to 6R decreases with the number of cycles and the drop is always greater when measured at lower deformations, i.e., to the left of the cycling curve, leading to a positive slope of the σ–ε transformation curve. This can be well explained if the 6R stabilization plays a significant role during cycling. If the transformation sequence is assumed to be the same in every cycle, zones that correspond to lower deformation values – to the left of the curve – remain in 6R for a longer fraction of the cycle than zones that correspond to higher deformation values, i.e., to the right of the curve. As more time is spent in 6R, more stabilization is observed and the stress drop is more pronounced. This is well observed in both described tests (see Figs. 2 and 3), the plots indicate higher stress drops for smaller amounts of transformed material after the same number of cycles. The inhomogeneous stabilization supports the hypothesis that the sequence of transformation is constant and repeats in each cycle, as regions of the sample that underwent more stabilization will transform at lower critical stresses in subsequent cycles.

In spite of the mentioned shift in the transformation stresses, hysteresis variation amplitude is kept below 3 MPa at 0.147 Hz. In other words, the sample was able to maintain a huge 120 MPa hysteresis for 1000 cycles, within $\pm 2\%$ stress variation. This behavior is unique and might be successfully used in damping applications.

At 0.147 Hz the behavior of the material improves dramatically when compared to 1.9×10^{-2} Hz. However, this frequency is still considerably lower than the main frequency experienced in seismic applications (about 1 Hz) [16]. To evaluate the behavior of the material in conditions close to real-life, a fresh sample with the same crystallographic orientation was submitted to cycling at 1 Hz on a MTS servo-hydraulic machine. The results are presented in Fig. 4.

At 1 Hz the amount of stabilization up to about 1000 cycles is lower than at 0.147 Hz. However, the difference in stabilization is not proportional to the difference in frequency. In order to check for the effect of possible self-heating of the specimen due to the work delivered in the hysteresis cycles, a thermocouple was added to the specimen. An asymptotic temperature increase of 6 K in the specimen was observed when cycling at 1 Hz. According to the Clausius–Clapeyron equation for the 18R–6R transformation such heating can produce a decrease of about 2.5 MPa in the transformation stresses, which remains very small compared with the stabilization values measured in Fig. 4c. At lower frequencies, sample heating is expected to be even smaller.

It can also be observed in Fig. 4b that after more than 2000 cycles at 1 Hz the curves degenerate significantly (see Section 4 for details). In spite of this hysteresis decrease it can be emphasized that the sample reached 5000 cycles without suffering fracture.

The behavior of the material up to about 1000 cycles at 1 Hz is outstanding, which encourages further research into its possible engineering uses.

It is well known from results in the literature [53,32] that 6R stabilization is a diffusive effect and that diffusion in CuZnAl alloys is already noticeable at room temperature. Thus, it is worth analyzing the effect of 18R–6R cycling at conditions sufficiently free from diffusion, as possible effects of the presence of precipitates might be visible. With this aim and in order to isolate the 18R–6R transformation from the β-18R transformation, a sample was completely transformed to 18R by mechanical stress at 303 K (see Fig. 5a), reaching a stress marked as point A in the curve. After that, it was cooled to 243 K under tension. When the temperature stabilized at 243 K, the load was removed but no retransformation to β was observed, as the test temperature was below the Austenite start temperature (A_s). The sample was then submitted

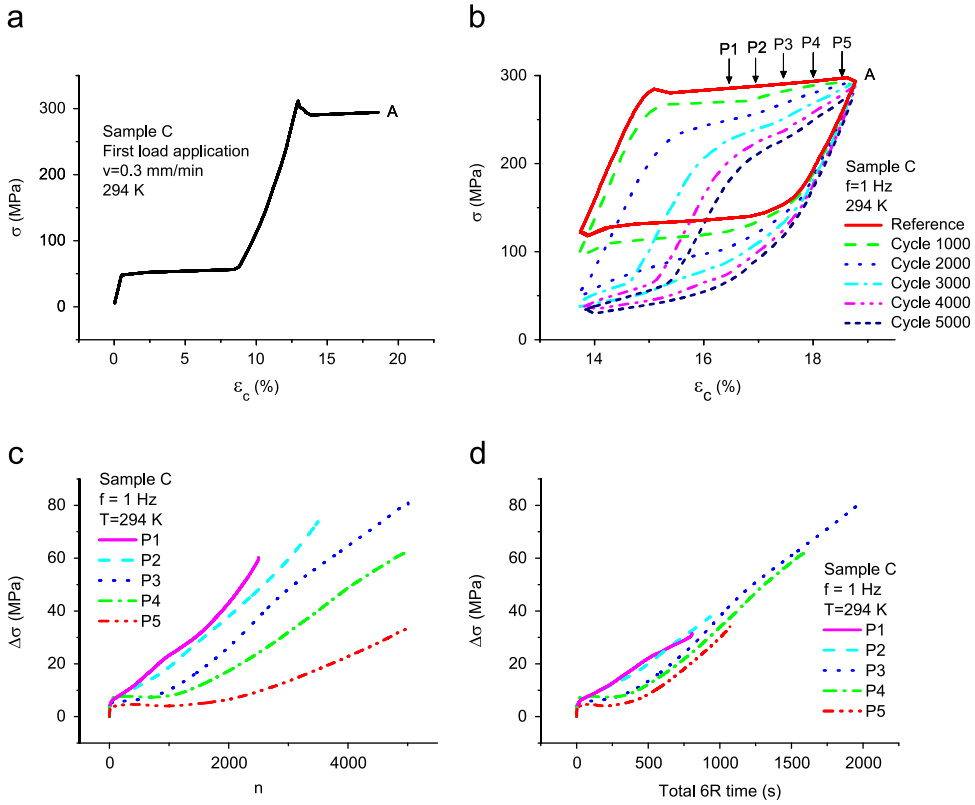

Fig. 4. Cycling test with sample C. (a) First load application. (b) Cycling at 294 K, 1 Hz. (c) Variation of 18R–6R transformation stress vs. number of cycles for different strain values. (d) Variation of 18R–6R transformation stress vs. accumulated 6R time. Crosshead displacement was used to calculate ε in all curves.

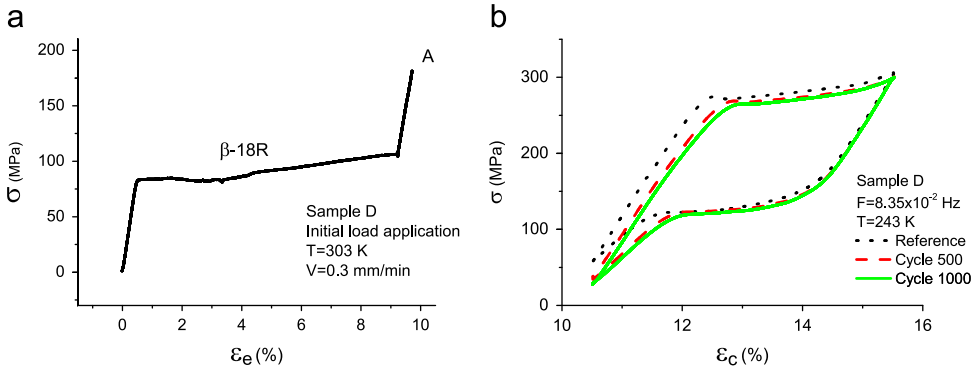

Fig. 5. (a) First load application (with extensometer) at 303 K; 18R is formed and elastically strained up to point A. (b) Cycling curves at 8.35×10^{-2} Hz (crosshead), $T=243$ K.

to 1000 mechanical cycles. The stress–strain shows a very slight variation after a few hundred cycles (see Fig. 5b). Considering that no slope is observed in the transformation stage after cycling, it is possible to ascertain that, if stabilization is minimized, the mechanical behavior during 18R–6R cycling with precipitates is strongly stable (see Fig. 5b).

Additional information can be obtained from the test shown in Fig. 5 if the critical transformation stresses to transform to 6R and retransform to 18R are obtained for different amounts of transformed 6R. This has been done and the corresponding shifts in these stresses, i.e. $\Delta\sigma=\sigma_r-\sigma_n$ for the transformation and retransformation stresses were also obtained. Results are briefly commented: σ^{18R-6R} decreases slightly but rapidly during the first cycles and a further decrease takes place at a slower rate. On the other hand, retransformation stresses (σ^{6R-18R}) increase during the first 40 cycles and then decrease during the rest of the cycling stage. Both results suggest that the slight decrease in hysteresis observed during the first stage of cycling can be attributed to the precipitate effect and a slight effect of dynamic stabilization might also be present after further cycling, although not strong enough to induce an evident slope at the transformation stage during cycling. On the whole, after 1000 cycles the hysteresis at this temperature decreased less than 3%, which means that if stabilization is minimized, very good mechanical stability can be obtained.

3.2. Study of quasistatic stabilization

Reported results on 6R stabilization under quasistatic conditions, concerning both stress drop and kinetic aspects have been reported for thermal treatments different from the one used here to introduce precipitates. Additionally, the time interval between the thermal treatment and the mechanical tests will also affect the concentration of vacancies at the start of the dynamic tests [63,45]. In order to have a reference for stabilization kinetics under static

conditions, at a concentration of vacancies close to the one used in cycled samples in the present manuscript, a sample was prepared to obtain partial information on the stabilization magnitude and kinetics with the same thermal treatment used for all samples. After the thermal treatment to introduce precipitates, the sample was kept at room temperature (about 295 K) for 2 days and tensile stressed at a low crosshead speed (0.3 mm/min), at a test temperature equal to 303 K. An 18R–6R cycle was interrupted at three different points so that different parts of the sample were kept in 6R for different time intervals (Fig. 6). The points where the cycle was interrupted during the second transformation are shown with arrows in Fig. 6, where only the 18R–6R part of the σ–ε curve is shown. The part of the sample that corresponds to the left of the first point was kept in 6R for a total of 9.36×10^4 s. Between the first and the second points, the sample was kept in 6R for 1.8×10^4 s. Between points two and three, the sample was kept in 6R for 3.6×10^3 s. The part of the sample that corresponds to the right of point 3 was kept in 6R for a very short time, less than 60 s. After this differential stabilization treatment, the sample was unloaded and submitted to two additional cycles. Results are seen in Fig. 6b, where nearly no recovery of the critical stress to obtain the 6R structure is visible.

The load was then completely removed from the sample, but the part of the sample that underwent the strongest martensite stabilization, i.e. the part that remained in 6R for the longest time, did not retransform back to β. After 9.72×10^4 s, the sample was submitted to a cycle (Fig. 7a). A significant slope is observed in the 18R–6R transformation stage, very similar to the slope observed before removing the load. This result suggests that the recovery of the 6R phase is not significant while the alloy is in the 18R phase. After this cycle, the sample was then heated to 333 K without any loads applied and thermally retransformed to β. After 1.08×10^4 s at 333 K, the sample was submitted to a new cycle (Fig. 7b). There is a significant difference in the 18R–6R transformation slope, which now basically occurs at constant stress. This result confirms that both the 18R and the 6R martensite recover very quickly when the alloy is in the β phase.

The results obtained in the aforementioned quasistatic experiment strongly suggest that, after stabilization of 6R, no recovery of the 18R–6R critical stresses is observed if the material remains in the 18R martensite. In order to confirm this relevant point, an additional experiment was performed after the same thermal treatment and using the same time period before stressing the sample. In this way the initial concentration of vacancies should be close to the previous one. A reference β–18R–6R cycle, here named cycle 1($N=1$), was performed at $T=303$ K and, after a second transformation up to 32% of 6R formation (point A marked at the graph), the strain was kept constant during 1.73×10^5 s. The sample was then unloaded down to point B (18R martensite). A following 18R–6R cycle (B–A–B), $N=3$, clearly showed stabilization (see Fig. 8), the maximum amount of stabilization was equal to 48 MPa. Deformation was kept fixed at point B (18R martensite) during 1.73×10^5 s and a further cycle, $N=4$, was performed (B–A–B). The obtained stress–strain curves corresponding to cycles 3 and 4, i.e., after stabilization in 6R at point A, and after keeping deformation fixed at point B, respectively, show an almost exact overlap. This result clearly shows that if the 6R martensite is stabilized, no recovery to a previous condition is obtained if the material is kept in 18R martensite. This result suggests that either the recovery kinetics of the 6R phase while in 18R is extremely slow or that it does not happen at all. In order to eliminate this ambiguity, further experiments are needed. If recovery does happen after a long time in 18R, it would have the potential to restore the original 18R–6R cycle, which could be beneficial to seismic damping, as the original

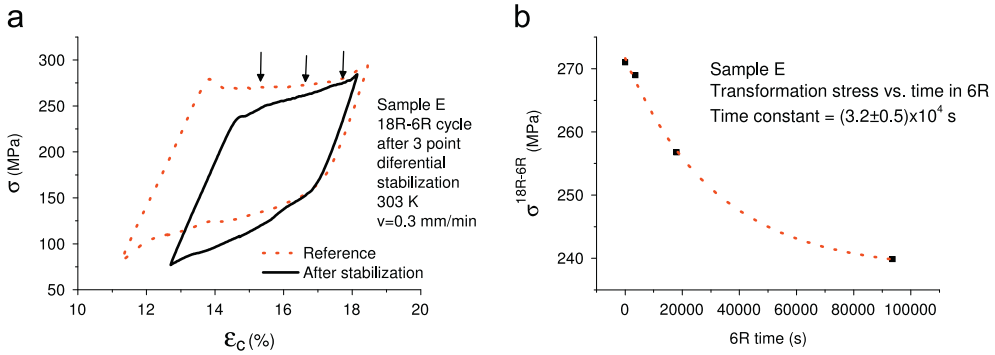

Fig. 6. (a) 18R–6R cycles before (reference) and after 6R stabilization. Arrows separate regions of the sample submitted to different time intervals at 6R (see text); (b) 18R–6R transformation stress (σ^{6R-18R}) vs. time in 6R (t_{6R}). The time constant obtained is $(3.2 \pm 0.5) \times 10^4$ s. Test temperature is 303 K.

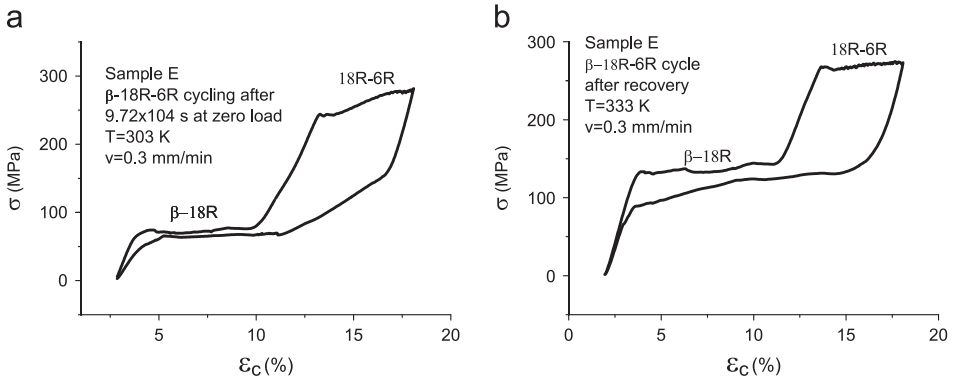

Fig. 7. (a) β–18R–6R cycle after 9.72×10^4 s at zero load obtained for sample E at 303 K (part of the sample had not previously retransformed to β and little, if any, recovery is observed); (b) β–18R–6R cycle after 1.08×10^4 s at 333 K (the sample had completely retransformed to β and full recovery is observed at the 18R–6R stage).

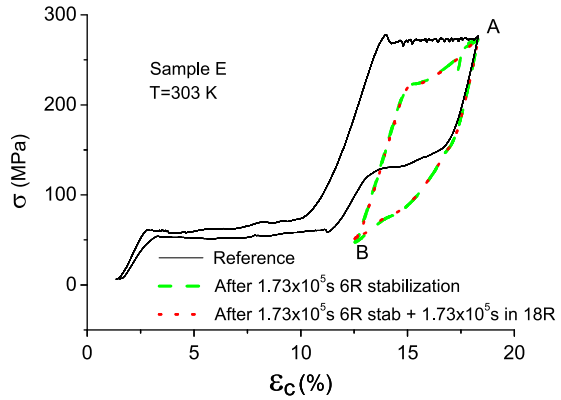

Fig. 8. β–18R–6R reference cycle (cycle 1) and 18R–6R cycles after stabilization. $T=303$ K, crosshead speed = 0.3 mm/min. Point A indicates the maximum strain reached during cycles 1 and 2. In cycle 2, the strain was kept fixed at point A for 1.73×10^5 s and the sample was unloaded down to point B. A following cycle ($N=3$) shows the effects of stabilization. Point B shows the position where the 18R–6R cycle was interrupted for another 1.73×10^5 s, keeping the sample in 18R. A final cycle ($N=4$) shows that the recovery of the 6R phase while the sample is in the 18R phase is negligible, even after 1.73×10^5 s.

18R–6R cycle might be restored between a major earthquake and its aftershocks. However, even if recovery does not happen at all, our results show that the material can be submitted to about 2000 cycles before 6R dynamic stabilization seriously compromises damping capacity, in the frequency range expected during an earthquake. This number of cycles is more than enough for a single major earthquake and its fore and aftershocks.

In order to have an additional reference for stabilization kinetics under static conditions, at a concentration of vacancies smaller than the one used in cycled samples in the present manuscript, a sample was prepared with the same thermal treatment used for all samples. After the thermal treatment to introduce precipitates, the sample was kept at room temperature (about 295 K) for 6.05×10^5 s and strained at a low crosshead speed (0.3 mm/min), at a test temperature equal to 303 K. A reference cycle up to about 48% of full 6R transformation was performed (Fig. 9a) and unloaded down to point A. A following 18R–6R cycle starting from point A was interrupted at approximately 21% of full 6R transformation (the arrow in Fig. 9b indicates the interruption point). Only the 18R–6R cycles are shown in Fig. 9b. After 9.0×10^4 s, the 18R–6R cycle was completed and another 18R–6R cycle was performed in order to measure the stabilization. After that, another 18R–6R cycle was started and interrupted at exactly the same point (about 21% of full 6R transformation) for an additional 2.376×10^5 s. The stabilized part of the sample remained in 6R for a total of 3.276×10^5 s. An 18R–6R cycle was then performed to measure the accumulated stabilization and the load was completely removed (Fig. 9c). Critical stresses to obtain 6R (σ^{18R-6R}) are plotted as a function of time in Fig. 9d.

4. Discussion

The results obtained indicate that 18R–6R cycling at low frequencies leads to an inhomogeneous stress–strain behavior in which the critical stresses to form 6R decrease a higher amount for those regions of the sample which first transform to 6R. This behavior can be understood if stabilization of 6R phase is considered. Several authors have analyzed different aspects of this stabilization and we will briefly mention significant points of this effect, mainly presented by Saule et al.[32,53,54]: (a) the critical stress to form 6R is independent of previous stabilization of 18R, (b) further stabilization of 6R can be obtained after 18R is fully stabilized and (c) a correspondence between the fct tetragonality and the amount of stabilization is found for 18R while the 6R phase can be described as a nearly cubic phase with a small tetragonality which is not affected by the stabilization of the phase. Additionally, as it was considered in the introduction, it has been accepted that diffusion in 18R martensite can be well explained by the interchange between Cu and Zn atoms, which is clearly a thermally activated effect, enhanced if the amount of vacancies increases [2,55,45]. It has been explained that the 6R structure, being a more symmetric structure if compared with 18R martensite, has more planes useful for the atomic interchange, which enables further stabilization of 6R even if the 18R martensite is previously stabilized up to its saturation [53]. For further information, Fig. 1 in the paper by Saule et al. [32] nicely shows the unit cell of a face centered tetragonal (f.c.t) martensite with the sublattice sites I–IV inherited from the β phase. In that figure, a type (1 1 1) basal plane is shown, as well as the Miller indexes corresponding to the f.c.t cell and to the orthorhombic structure. The main contribution to the stabilization of the martensite in these alloys has been reported to be the disordering of Cu and Zn atoms between sites corresponding to sublattices I, II and III, IV, respectively. In fact, the interchange takes place between Cu and Zn atoms which occupy neighbor sites which indeed belong to neighboring (0 0 1) planes of the basic f.c.t. lattice [32].

The evolution of the stress–strain curves in Fig. 2 can be rationalized if the 6R structure stabilizes while cycling, the magnitude of stabilization being dependent on the time interval each part of the sample remains in 6R. Moreover, Figs. 2 and 4d indicate that the stabilization of each part of the sample, measured as the absolute value of the decrease in the critical stress to transform to 6R can be well described by a linear behavior as a function of the time interval in which the considered material volume spends in this structure. The main and significant point to notice here is that one physical mechanism, i.e. 6R stabilization, plays the most significant role in the mechanical evolution during pseudoelastic cycling. The amount of 6R stabilization in quasistatic experiments [53] depends on the temperature and on the initial concentration of vacancies. In fact Saule et al. reported that after step quenching at 573 K is was not possible to measure the retransformation from 6R to 18R and maximum 6R stabilization amounts close to 60 MPa (critical resolved shear stresses) were obtained for samples step quenched at 473 K and tested after the stabilization to saturation of 18R and for samples step quenched at 373 K and immediately transformed to 6R. The concentration of vacancies is a relevant parameter in this type of experiment and cannot be expected to be the same in samples cycled in the present work and in those reported in the literature. Due to this fact it is necessary to compare the amount of stabilization obtained after cycling (for example in Fig. 2) and in the quasistatic tests corresponding to a concentration of vacancies close to the one used in dynamic tests (Figs. 6–8). In the experiment of Fig. 6 the strain was kept fixed at different amounts of transformed 6R, leading to well defined time intervals at 6R of each part of the sample, i.e., 3.6×10^3 s, 1.8×10^4 s, and 9.36×10^4 s, respectively. A simple exponential fit gives a time constant equal to $3.2\pm0.5\times10^4$ s, and the stabilization amount reaches 30 MPa after 9.36×10^4 s. An interesting point here is that during unloading, a slope is obtained at the 6R–18R retransformation stage. This behavior is somehow unexpected and at variance with similar experiments performed for stabilization of the 18R structure, where clear steps in the retransformation stress link the plateaus of each part of the curve [42]. Although further research might be necessary to better understand this result, preliminary in situ observations have shown that the 6R–18R retransformation front

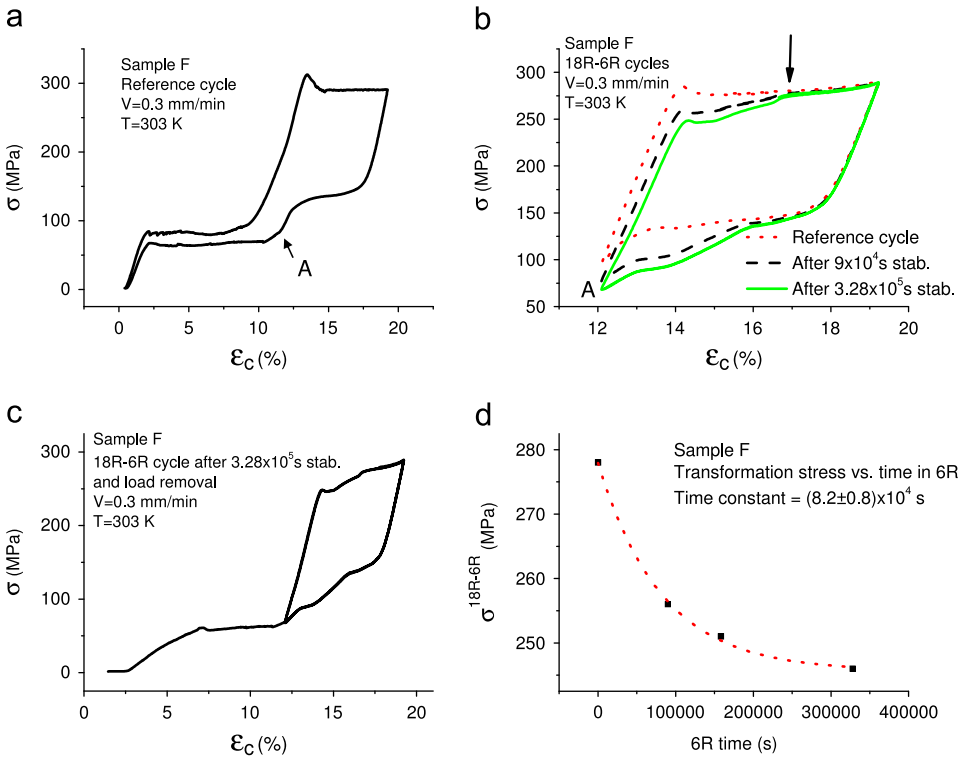

Fig. 9. (a) β–18R–6R reference cycle, (b)18R–6R cycles after stabilization, (c) load removal. All cycles were performed at 303 K and the crosshead speed used was 0.3 mm/min and (d) transformation stress σ^{18R-6R} vs. time at 6R (t_{6R}), from which a time constant $(8.2 \pm 0.8) \times 10^4$ s is obtained.

has a considerable length, which leads to a retransformation stress which shows contributions from neighbor regions stabilized during different time intervals. This hypothesis is further supported by the result of the quasistatic stabilization test performed after keeping the sample a larger time in the β phase before transforming to martensite (Fig. 9).

From the quasistatic experiments performed to evaluate the stabilization amount and kinetics with a concentration of vacancies close to the concentration at the start of the dynamic tests, it can be observed that the stabilization magnitude reaches 30 MPa after 9.36×10^4 s and of course smaller values for shorter time intervals. These values are considerably smaller than the stabilization magnitude which is obtained after cycling, at similar time intervals in 6R (see Figs. 2 and 4d). This strong difference in stabilization kinetics between quasistatic and dynamic experiments has also been found after the analysis of pseudoelastic cycling between the β phase and the 18R martensite [56]. In the latter case it was possible to predict the mechanical behavior by considering an enhanced kinetics of 18R stabilization under dynamic conditions if compared with static stabilization. The origin of this enhanced kinetics was attributed to the creation of point defects during cycling. The annihilation of dislocations was the mechanism proposed. Although there is not enough data concerning the microstructure evolution during 18R–6R cycling, both martensitic structures differ mainly in the stacking fault and the 6R structure is in fact a more symmetric phase, with a tetragonality close to 1. This fact allows us to consider that the phase is nearly cubic [54], and it is reasonable to accept the same mechanism as the origin of an extra amount of vacancies during cycling through the 18R–6R transition. Additionally, results concerning the creation of vacancies during fatigue in Cu have been initially reported by Polák [64] and experimental results obtained after β–18R pseudoelastic cycling at low temperatures indicated that an extra amount of vacancies are added to the initial amount [57,58]. Moreover, we have considered that the rapid movement of interfaces during β–18R cycling enhances diffusional processes like the stabilization of 18R martensite due to the difference in the concentration of vacancies between β and 18R [65]. Although the movement of interfaces is expected to have an effect on the vacancies present in the material, cycling between 18R and 6R involves martensitic structures which only differ in the stacking of basal planes, as the distance between the first and second neighbor atoms is the same or very similar in both structures. Then, a significant difference in the concentration of vacancies between both martensites should not be expected. Thus, the generation of vacancies seems to be the most plausible mechanism to explain the strong increase in stabilization of the 6R structure during dynamic tests in comparison with quasistatic stabilization tests.

According to the present results, an interesting analogy is observed if we consider both rapid pseudoelastic cycling between austenite and 18R martensite and cycling between both martensites, 18R and 6R. In both cases the stress-strain evolution can be rationalized by taking into consideration a well-understood physical mechanism under quasistatic conditions, i.e., the stabilization of 18R or 6R, respectively, although with different kinetics if slow and rapid cycling are compared. However, one significant difference is to be noticed between both situations. It has been shown that the prediction of the mechanical evolution during β–18R cycling can be well explained by the presence of two physical mechanisms, i.e. the stabilization of 18R martensite and the recovery of the β phase to its original order [56]. Moreover, diffusion in β is clearly easier than in 18R mainly due to the difference in the concentration of vacancies. On the other hand, if cycling between 18R and 6R is considered, the stabilization of 6R modifies the critical resolved shear stresses involved, shifting the whole cycle to smaller stresses. However, when the material is in the 18R phase no such mechanism as the recovery of β is to be expected, as commented below. This fact leads to relevant differences between the mechanical behavior in β–18R cycling and 18R–6R cycling and also if cycling up to 6R formation is considered, starting from β or from 18R.

Concerning the role of 18R in the pseudoelastic 18R–6R cycling, the quasistatic experiments shown in Figs. 6 and 8, also performed with the same amount of vacancies as the dynamic tests of the present manuscript, show that after the 6R stabilization of different portions of the sample during selected time intervals, if the sample is kept in the 18R phase, no change in the critical stresses to obtain 6R are observed. This fact has been observed by Saule et al. in quasistatic experiments for a different amount of vacancies [53]: 18R stabilization does not affect the critical stresses to obtain 6R but the stabilization of 6R also stabilizes the 18R phase. This fact is understandable if the same type of atom pair interchanges play the main role in both stabilization mechanisms and the asymmetric influence is just a consequence of the fact that 6R has more planes available to perform the atomic interchanges (including some planes at an angle relative to the basal plane), if compared with the 18R structure.

It is clear from the results obtained here that the mechanical evolution during 18R–6R cycling is mainly affected and explained by the stabilization of the 6R structure. The stabilization is enhanced by rapid cycling when the same time elapsed in 6R is considered for a given region of the specimen. It is believed that this rapid stabilization is related to the number of cycles, i.e. the number of times the interface crosses the region under consideration. Results reported in the literature, obtained from quasistatic tests, show that saturation is usually obtained after stabilization in the 6R martensite, although in some cases this effect is not observed (see Fig. 3 in [53]). The stabilization curves obtained in the present manuscript under dynamic conditions have not shown the saturation phenomena in a clear way. The 6R stabilization observed during dynamic tests might be an obstacle for applications. However, if the frequency of cycling is increased up to values close to the reported frequencies in seismic events, the time interval the material spends in 6R decreases noticeably, leading to small variations in the stress–strain curves (see Fig. 4) during the required working time, which is an extremely interesting result.

As stabilization is a diffusive phenomenon, decreasing the temperature should inhibit this mechanism, highlighting the effect of precipitates on the mechanical behavior after cycling. The results obtained in the present paper (Fig. 5) show that no significant inhomogeneous stabilization is evident after cycling at a temperature lower than room temperature ($T=273$ K). The obtained result also indicates that a slight homogeneous decrease in the critical stresses to transform to 6R is in fact observed after cycling. The stress to retransform to 18R slightly increases with the number of cycles, leading to a decrease of the hysteresis of only 6% after 1000 cycles at a frequency = 1 Hz. No doubt this result is strongly indicative that if stabilization is minimized due to higher frequencies, the stress–strain behavior is rather stable if nanoprecipitates are introduced.

It is convenient to emphasize that the main role that precipitates play is the hardening of the 6R martensite, as already demonstrated [38]. In this way, a higher amount of reversible deformation is reached in each cycle. However, considering the effect of 6R stabilization on the mechanical evolution, it is valid to question if the introduced nanoprecipitates have an additional consequence on the amount of stabilization. No reported results analyze the effect of precipitates on the 6R stabilization. Nevertheless, an interesting result was reported by García et al. concerning the effect of γ precipitates on the stabilization of 18R martensite in CuZnAl alloys of composition very close to the one used in the present work [66]. These authors found a slight decrease in the amount of stabilization for samples where precipitates had been introduced. This inhibition of the stabilization effect was attributed to a decrease in the amount of vacancies, which might occur due to the structural vacancies present in the precipitates and to dislocations formed around them, which act as vacancy sinks. Further research is needed to verify if these mechanisms are also valid when 6R stabilization is considered, although it is reasonable to expect a similar effect if we consider that vacancies play a significant role facilitating the pair interchange of Cu and Zn atoms both during 18R and 6R stabilization.

Finally, a question arises if potential applications using the 18R–6R phase transition are to be taken into account: is it convenient to consider 18R–6R cycling or might cycling from the β austenitic phase give better results? One of the consequences of cycling between 18R and 6R might be the overlap between the retransformation stress σ^{6R-18R} and the critical stress $\sigma^{18R-\beta}$ required to retransform the non-transformed 18R, as it is observed in the last cycles of Fig. 4b. This leads to a decrease in hysteresis. Present results strongly indicate that if the required frequency is high enough, the stabilization of 6R, in spite of playing the main role on the mechanical evolution, does not have enough time to be a deleterious contribution. However, if the required frequency were not high enough (lower than about 10^{-2} Hz) to use only the 18R–6R transformation, the full β–18R–6R cycle might be used instead, which activates β ordering while the material is in the β phase, contributing to a recentering mechanism of an application in addition to doubling the obtained deformation as measured in the material.

5. Conclusions

The effect of pseudoelastic cycling through the martensite to martensite 18R–6R transition in CuZnAl single crystals with nanoprecipitates has been described. Variations of the critical stresses to transform and 18R–6R hysteresis have been mainly explained by the effect of 6R stabilization. Recovery of the 18R phase does not take place during 18R–6R cycling.

The stabilization phenomenon under dynamic conditions is complex and cannot be easily described by existing models. Care must be taken not to oversimplify dynamic martensite stabilization, as the behavior under dynamic conditions might be very different from static conditions, such as reported by Yawny et al. [56] for β–18R cycling in CuZnAl SMA single crystals.

Even though material properties change as a function of the time spent in martensite, the specific conditions found in a single seismic event should not cause significant changes in mechanical properties. This occurs for the following reasons: (1) The rate at which material properties change is low enough for possible seismic damping uses. Given the expected number of cycles in a seismic event and the fundamental frequency of common civil structures, the total amount of time the material is expected to spend in martensite is relatively low. (2) The total number of expected cycles in a seismic event, including aftershocks, should not be higher than a few hundred cycles.

Compared to NiTi, second stage martensitic transformation in CuZnAl has much greater hysteresis, which should result in superior damping, leading to devices that are cheaper and have superior performance.

Compared to newly invented Fe-base superelastic alloys, the hysteresis of the second stage martensitic transformation in CuZnAl single crystals is smaller than in the textured alloy [34] but comparable to the single crystal [36], up to 100 cycles. Dynamic stabilization seems to be faster in Fe-based single crystals than in CuZnAl. Unfortunately, no information is available concerning Fe-based single crystals for the number of cycles studied in this work, i.e. up to 5000 cycles, so a complete comparison is not possible. However, based on currently available information, CuZnAl single crystals are easier to manufacture, have comparable hysteresis and possibly slower dynamic stabilization than Fe-base

single crystals. CuZnAl single crystals have, thus, a unique combination of characteristics, making it a very interesting candidate for seismic damping.

From the present results, the mechanical behavior is outstanding at or above 1.47×10^{-1} Hz, and it is possible to reach 2000 cycles with little stabilization. If stabilization is tolerated, the material might be used up to 5000 cycles or more, with very little temperature dependence. As real-life vibration frequencies are usually above 1.47×10^{-1} Hz in seismic events, the material could be successfully used in damping applications. The worst-case scenario would be a reduction in hysteresis, even though the number of cycles expected in anti-seismic applications is not enough for significant 6R stabilization to happen. For seismic damping in civil structures (frequencies around 1 Hz, 200 cycles), the measured hysteresis loss is smaller than 3%. More research is required, but the results show that the material studied has outstanding properties for damping devices in civil structures.

Acknowledgments

Argentina (Project PIP 112 201101 00 513) and SECTyP UNCUYO-Argentina (Project 06/C387) contributed with financial support. The first author would like to express his gratitude for the doctoral fellowship provided by CONICET-Argentina. Mrs. T. Carrasco helped with the preparation of alloys, Mr. C. Gómez helped with sample preparation, Mr. P. Riquelme provided technical support with testing machines and Mr. R. Stuke improved the system to grow single crystals. We thank Dr. A. Yawny for the fruitful discussions regarding the results in this study.

References

[1] Z. Saburi, Y. Inada, S. Nenno, N. Hori, J. Phys. C4–43 (1982) 633–638.
[2] M. Ahlers, Prog. Mater. Sci. 30 (1986) 135–186.
[3] C.M..Friend, A.P..Miodownik, in: Proceedings of the Ph. Transform.'87, Cambridge, UK, 1987, pp. 276–278.
[4] H..Sakamoto K..Shimizu, in: Proceedings of the Ph. Transform.'87, Cambridge, UK, 1987, pp. 282–284.
[5] M. Ahlers, J.L. Pelegrina, Acta Metall. Mater. 40 (1992) 3213–3220.
[6] K. Otsuka, C.M. Wayman, Shape Memory Materials, in: K. Otsuka, C.M. Wayman (Eds.), Cambridge University Press, Cambridge, UK, 1998, pp. 27–48.
[7] O. Ben Mekki, F. Auricchio, Int. J. Non-Linear Mech. 46 (2011) 470–477.
[8] V. Torra, A. Isalgue, C. Auguet, G. Carreras, F.C. Lovey, P. Terriault, L. Dieng, Appl. Mech. Mater. 82 (2011) 539–544.
[9] A.M. Sharabash, B.O. Andrawes, Eng. Struct. 31 (2009) 607–616.
[10] S. Casciati, L. Faravelli, Comput. Struct. 86 (2008) 330–339.
[11] Y. Zhang, S. Zhu, J. Eng. Mech. 134 (2008) 240–251.
[12] M.S. Alam, M.A. Youssef, M. Nehdi, Can. J. Civ. Eng. 34 (2007) 1075–1086.
[13] V. Torra, A. Isalgue, F. Martorell, P. Terriault, F.C. Lovey, Eng. Struct. 29 (2007) 1889–1902.
[14] C. Auguet, A. Isalgué, F.C. Lovey, F. Martorell, V. Torra, J. Therm. Anal. Calorim. 88 (2007) 537–548.
[15] R. Desroches, B. Smith, J. Eartquake Eng. 8 (2004) 415–429.
[16] V. Torra, A. Isalgue, C. Auguet, G. Carreras, F.C. Lovey, H. Soul, P.J. Terriault, J. Mater. Eng. Perform. 18 (2009) 738–745.
[17] R. DesRoches, J. McCormick, M. Delemont, J. Struct. Eng. 130 (2004) 38–46.
[18] T. Saburi, in: K. Otsuka, C.M. Wayman (Eds.), Shape Memory Materials, Cambridge University Press, Cambridge, UK, 1998, pp. 49–96.
[19] A. Yawny, M. Sade, G. Eggeler, Z. Metallkd. 96 (2005) 608–618.
[20] A. Yawny, J. Olbricht, M. Sade, G. Eggeler, Mater. Sci. Eng., A 481–482 (2008) 86–90.
[21] A. Isalgue, V. Torra, A. Yawny, F.C. Lovey, J. Therm. Anal. Calorim. 91 (2008) 991–998.
[22] J. Olbricht, A. Yawny, A.M. Condó, F.C. Lovey, G. Eggeler, Mater. Sci. Eng., A 481–482 (2008) 142–145.
[23] S. Montecinos, A. Cuniberti, J. Alloys Compd. 457 (2008) 332–336.
[24] S. Montecinos, A. Cuniberti, A. Sepúlveda, Mater. Charact. 59 (2008) 117–123.
[25] J.F. Beltran, C. Cruz, R. Herrera, O. Moroni, Eng. Struct. 33 (2011) 2910–2918.
[26] C.A. Biffi, P. Bassani, A. Tuissi, M. Carnevale, N. Lecis, A.L. Conte, B. Previtali, Funct. Mater. Lett. 5 (2012), art. no. 12500142.
[27] J.L. Pelegrina, M. Ahlers, Acta Metall. Mater. 40 (1992) 3205–3211.
[28] P. Wollants, J.R. Ross, L. Delaey, Prog. Mater. Sci. 37 (1993) 227–288.
[29] L. Delaey, J. Janssen, J. Van Humbeeck, J. Luyten, A. Deruyttere, in: Proceedings of the ICOMAT, 1979, Cambridge, MA, 1979, pp. 645–648.
[30] G. Barceló, M. Ahlers, R. Rapacioli, Z. Metallkd. 70 (1979) 732–738.
[31] K. Takezawa, T. Izumi, H. Chiba, S. Sato, J. Phys. C4–43 (1982) 819–824.
[32] F. Saule, M. Ahlers Acta, Metall. Mater. 43 (1995) 2373–2384.
[33] V. Torra, C. Auguet, G. Carreras, L. Dieng, F.C. Lovey, P. Terriault, Mater. Sci. Forum 706–709 (2012) 2020–2025.
[34] Y. Tanaka, Y. Himuro, R. Kainuma, Y. Sutou, T. Omori, K. Ishida, Science 327 (2010) 1488–1490.
[35] T. Omori, K. Ando, M. Okano, X. Xu, Y. Tanaka, I. Ohnuma, R. Kainuma, K. Ishida, Science 333 (2011) 68–71.
[36] P. Krooss, T. Niendorf, I. Karaman, Y. Chumlyakov, H.J. Maier, Funct. Mater. Lett. 4 (2012), art. no. 1250045.
[37] A. Cuniberti, R. Romero, Mater. Sci. Eng., A 273–275 (1999) 362–365.
[38] F.D.C. Bubani, M. Sade, F. Lovey, Mater. Sci. Eng., A 543 (2012) 88–95.
[39] J. Janssen, J. Van Humbeeck, M. Chandrasekaran, N. Mwamba, L. Delaey, J. Phys. C4–43 (1982) 715–720.
[40] G. Scarsbrook, J.M. Cook, W.M. Stobbs, Metall. Trans. A 15A (1984) 1977–1986.
[41] A. Abu Arab, M. Chandrasekaran, M. Ahlers, Scr. Metall. 18 (1984) 709–714.
[42] A. Abu Arab, M. Ahlers, Acta Metall. 36 (1988) 2627–2638.
[43] J.L. Pelegrina, M. Ahlers, Mater. Sci. Eng. A358 (2003) 310–317.
[44] S. Kustov, J. Pons, E. Cesari, J. Van Humbeeck, Acta Mater. 52 (2004) 4547–4559.
[45] M. Stipcich, R. Romero, Mater. Sci. Eng., A 437 (2006) 328–333.
[46] A. Cuniberti, R. Romero, M. Stipcich, J. Alloys Compd. 472 (2009) 162–165.
[47] M. De Graef, J. Van Humbeeck, M. Andrade, L. Delaey, Scr. Metall. 19 (1985) 643–646.
[48] L. Delaey, T. Suzuki, J. Van Humbeeck, Scr. Metall. 18 (1984) 899–903.
[49] T. Suzuki, R. Kojima, Y. Fujii, A. Nagasawa, Acta Metall. 37 (1989) 163–168.
[50] K. Otsuka, X. Ren, Mater. Sci. Eng. A312 (2001) 207–218.
[51] X. Ren, K. Otsuka, Nature 389 (1997) 579–582.
[52] Y. Hashiguchi, H. Higuchi, I. Matsui, T. Niitani, H. Tokunoh, Y. Ikai, in: Proceedings of the ICOMAT 1986, Nara, Japan, 1986, pp. 832–837.
[53] F. Saule, A. Tolley, M. Ahlers, Scr. Metall. Mater. 24 (1990) 363–368.
[54] F. Saule, M. Ahlers, F. Kropff, E.B. Rivero, Acta Metall. Mater. 40 (1992) 3229–3238.
[55] M..Ahlers, in: Proceedings of the ICOMAT 1986, Nara, Japan, 1986, pp. 786–793.
[56] A. Yawny, F.C. Lovey, M. Sade, Mater. Sci. Eng., A 290 (2000) 108–121.
[57] J. Malarría, M. Sade, F.C. Lovey, Z. Metallkde. 87 (1996) 953–962.
[58] M. Sade, J.Malarría, A. Yawny, F.C. Lovey, in: Proceedings of the XVIII Conference of Applied Crystallography, Wisla, Poland, 2000, pp.153–170.
[59] F.C. Lovey, R. Rapacioli, M. Chandrasekaran, Phys. Status Solidi A 68 (1981) K105–K111.
[60] F.C. Lovey, V. Torra, A. Isalgué, D. Roqueta, M. Sade, Acta Metall. Mater. 42 (1994) 453–460.
[61] F.C. Lovey, G. Van Tendeloo, J. Van Landuyt, M. Chandrsekaran, S. Amelinckx, Acta Metall. 32 (1984) 879–886.
[62] A.J. Bradley, C.H. Gregory, J. Inst. Met. 51 (1933) 131.
[63] W. Salgueiro, R. Romero, A. Somoza, M. Ahlers, Phys. Status Solidi A 138 (1993) 111–118.
[64] J. Polák, Scr. Metall. 4 (1970) 761–764.
[65] J.L. Pelegrina, M. Rodriguez de Rivera, V. Torra, F.C. Lovey, Acta Metall. Mater. 43 (1995) 993–999.
[66] J. García, J. Pons, E. Cesari, Mater. Res. Bull. 31 (1996) 709–715.